NANO LETTERS

LETTER

pubs.acs.org/NanoLett

PbSe Nanocrystal-Based Infrared-to-Visible Up-Conversion Device

Do Young Kim, Kaushik Roy Choudhury, Jae Woong Lee, Dong Woo Song, Galileo Sarasqueta, and Franky So*

Department of Materials Science and Engineering, University of Florida, Gainesville, Florida 32611-6400, United States

Supporting Information

ABSTRACT: Low-cost hybrid up-conversion devices with infrared sensitivity to 1.5 μm were obtained by integrating a colloidal PbSe nanocrystal near-infrared sensitizing layer on a green phosphorescent organic light emitting diode. A ZnO nanocrystal hole blocking layer is incorporated in the devices for keeping the device off in the absence of IR excitation. The maximum photon (1.3 μm)-to-photon (0.52 μm) conversion efficiency is 1.3%. The extension (until 1.5 μm) of the near-infrared wavelengths, which can be converted to visible light, may be able to improve night vision.

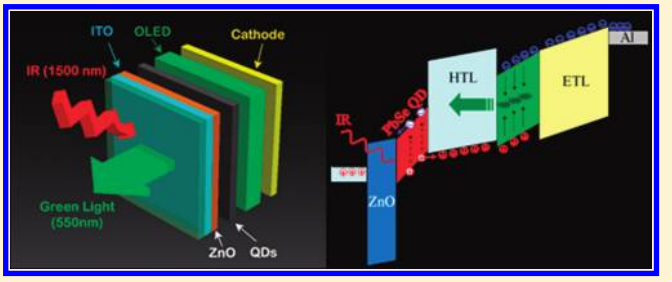

KEYWORDS: Up-conversion, infrared, PbSe, OLED, quantum dot, ZnO

Up-conversion devices have attracted a great deal of research interest because of their potential applications in night vision, range finding, and security as well as semiconductor wafer inspections.[1−4] Early near-infrared (NIR) up-conversion devices were made by integrating an infrared photodetector with a visible light emitting device.[5−7] However, fabrication of infrared-to-visible up-conversion devices based on inorganic compound semiconductors is challenging because of the lattice mismatch between the two types of semiconductor materials used for photodetectors and light emitting diodes. Because of the high costs of epitaxial grown inorganic devices, these devices are only suitable for small area applications. Recently, optoelectronic devices based on organic materials have received a lot of attention because of their compatibility with large area manufacturing. Up-conversion devices using organic semiconductors have previously been demonstrated. These devices can be realized by integrating an organic light emitting diode (OLED) with an organic photodetector.[8,9] However, the devices showed very low photon-to-photon conversion efficiencies, typically less than 0.05%. The low conversion efficiencies were due to the low efficiency OLEDs as well as low efficiency photodetectors. More recently, we have reported improved all-organic up-conversion devices[10] by integrating a *fac*-tris(2-phenylpyridinato)iridium-(III) ($Irppy_3$) phosphorescent OLED and a tin phthalocyanine (SnPc):C_{60} bulk heterostructure NIR photodetector. Compared to the earlier devices, these devices showed a significantly higher photon-to-photon conversion efficiency of 2.7% due to the high efficiency phosphorescent OLEDs used in the devices.

While there was progress made in device performance, these all-organic up-conversion devices have no infrared sensitivity beyond 1 μm. Detecting photons at long wavelengths requires low band gap inorganic semiconductors. Ban et al. reported a hybrid organic/inorganic up-conversion devices by integrating an OLED with an InGaAs/InP photodetector with sensitivity up to 1.5 μm.[11,12] However, the photon-to-photon conversion efficiency was only 0.25%. In addition to low efficiencies, the hybrid up-conversion devices are expensive to fabricate because the device fabrication is only compatible with small substrate size wafer processing. In this work, we demonstrated a low-cost up-conversion device with infrared sensitivity up to 1.5 μm using inorganic colloidal PbSe nanocrystals as a NIR sensitizer. PbSe nanocrystals were chosen because their optical absorption can be tuned from 0.7 to 2.0 μm.[13−15]

The structure of our NIR-to-visible light up-conversion device is schematically shown in Figure 1a. Up-conversion devices were fabricated on patterned ITO substrates with a sheet resistance of 20 Ω per square. The ITO substrates were first cleaned with acetone and isopropanol in an ultrasonic cleaner and subsequently rinsed with deionized water, blown dry with N_2 gas, and treated with UV ozone. Following this, a 60 nm layer of ZnO nanocparticles was spin-coated on top of the ITO substrate and then annealed at 90 °C for 15 min in the ambient. The substrate was subsequently introduced into a nitrogen glovebox, and a 50 nm PbSe nanocrystal layer was spin-coated. The PbSe nanocrystal layer was then treated with a benzenedithiol (BDT) solution to improve electronic coupling between individual nanocrystals. This treatment renders the PbSe film insoluble. For the OLED part of the device, a 45 nm thick 1,1-bis[(di-4-tolylamino)phenyl]cyclohexane (TAPC) layer was used as a hole transporting layer (HTL), a 30 nm thick 4,4-*N*,*N*-dicarbazole-biphenyl (CBP) layer doped with $Irppy_3$ was used as an emitting layer, and tris[3-(3-pyridyl)-mesityl]borane (3TPYBM) (45 nm) was used as a hole blocker/electron transporting layer (ETL). LiF/Al (1 nm/100 nm) was used as the cathode. All layers in the up-conversion devices were vacuum

Received: March 2, 2011
Revised: April 6, 2011

   dx.doi.org/10.1021/nl200704h | *Nano Lett.* XXXX, XXX, 000–000

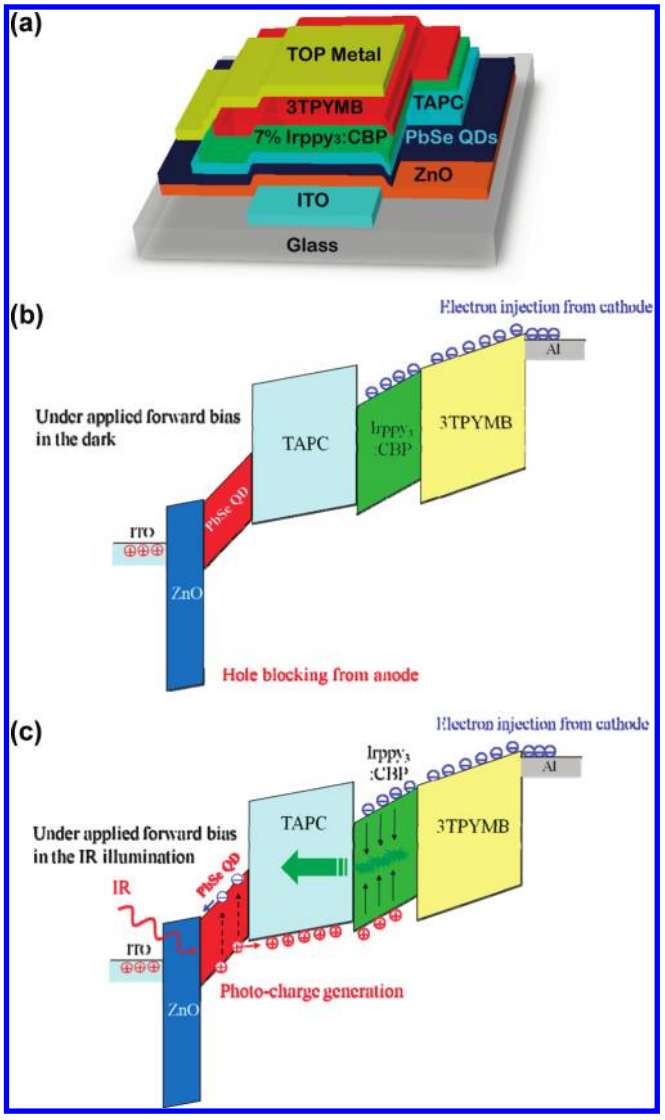

Figure 1. (a) Schematic cross-section view of PbSe QD infrared-to-green light up-conversion device, and schematic energy band diagrams of PbSe QD up-conversion devices (b) in the dark and (c) in the IR illumination.

deposited at a pressure of 1×10^{-6} Torr. The deposition rates were 0.5 and 1 Å/s for organic materials and aluminum, respectively. The area of the device is 0.04 cm^2. The ZnO nanocrystals were synthesized by a sol−gel process using precursors of zinc acetate and tetramethylammonium hydroxide (TMAH).[13] The PbSe nanocrystals were synthesized by decomposition of organometallic precursors as reported previously.[14] The PbSe nanocrystals were washed by precipitation and redispersion three times. Subsequently, the original long-chain oleate ligands on the nanocrystal surface were exchanged with octylamine, which is a shorter capping group. The surface-exchanged nanocrystals were washed and redispersed in chloroform.[14] All nanocrystal and polymer solutions were filtered using a 0.45 μm filter. Luminance−current−voltage (LIV) characteristics of the light up-conversion devices were measured using a Keithley 4200 semiconductor characterization system connected to a calibrated Si photodiode for photocurrent measurements. A 150 W ozone-free xenon arc lamp combined with 1.5G air mass filter, which produces the characteristic Class A spectrum, is coupled with the monochromator as a IR light source

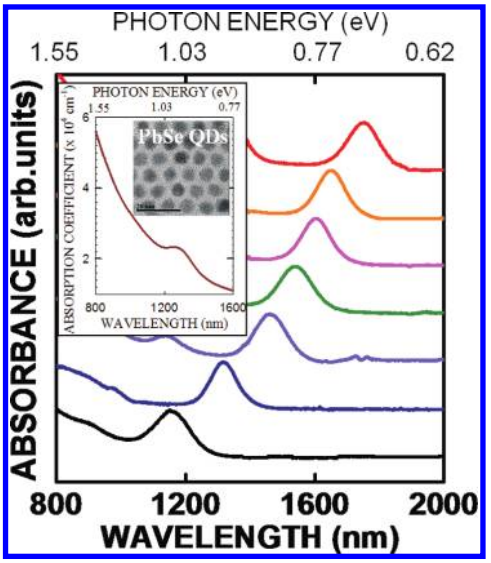

Figure 2. Absorbance spectra of PbSe nanocrystal with various sizes. (Inset: Absorption coefficient spectrum and TEM image of 50 nm thick PbSe QD film with 1.3 μm peak wavelength.)

to produce a monochromatic light in the wavelength range from 200 to 2800 nm. The devices were not encapsulated, and the measurements were carried out at room temperature under an ambient atmosphere.

Here, these up-conversion devices as shown in Figure 1a are basically conventional OLEDs with a PbSe nanocrystals IR sensitizing layer. For an OLED functioning as an up-conversion device, the key is to keep the device off when there is no NIR irradiation. To keep the device off when it is not under NIR irradiation, hole injection from the ITO anode should be suppressed under forward bias. In an OLED with a PbSe sensitizing layer under forward bias, holes are readily injected into the device from the ITO electrode through the PbSe layer. These injected holes turn on the OLED without incident NIR light. To keep the device off while the device is under forward bias, our strategy is to block hole injection from the ITO anode as shown in Figure 1b. Here, we used colloidal ZnO nanoparticles to form a hole-blocking layer (HBL) between the ITO anode and the PbSe layer. The ZnO HBL blocks hole injection from the ITO anode under forward bias due to its large band gap (3.4 eV) and deep valence band edge (7.6 eV). Upon photoexcitation, the photogenerated holes in the PbSe NIR sensitizing layer are injected through the HTL and into the emitting layer of the OLED and recombine with electrons injected from the cathode to give off visible light as illustrated in Figure 1c.

Figure 2 shows the absorbance spectra of different PbSe nanocrystals in solution. The absorption peak varies from 1150 nm for 3 nm size nanocrystals to 1750 nm for 6 nm size nanocrystals. The absorption spectra of PbSe nanocrystal films show similar absorbance spectra of PbSe nanocrystals in solution near the absorption peaks. The absorption coefficient at the peak wavelengths of PbSe nanocrystals films used in this study is about of 2.5×10^4 cm^{-1}. As-synthesized PbSe nanocrystals have poor carrier transporting properties due to the long oleic acid capping group. To use PbSe nanocrystals in the up-conversion devices, the oleic acid capping group needs to be replaced by a shorter capping group. Recently, we have demonstrated that the carrier transporting properties can be significantly enhanced if the long

dx.doi.org/10.1021/nl200704h |*Nano Lett.* XXXX, XXX, 000–000

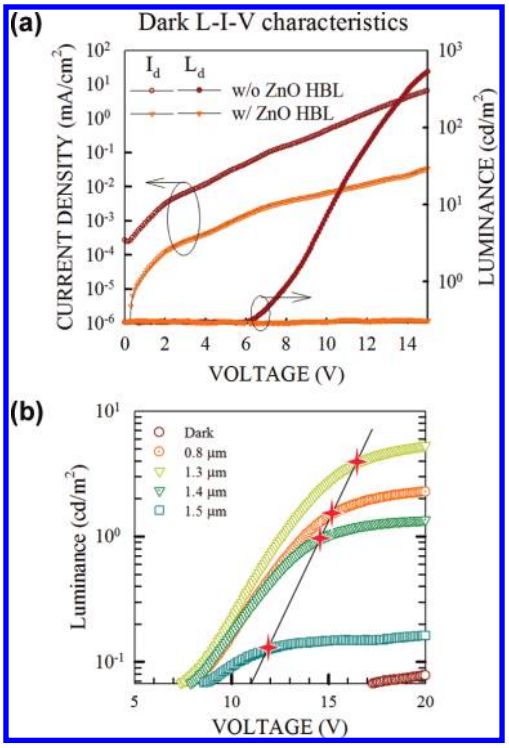

Figure 3. (a) Dark $L-I-V$ characteristics of PbSe up-conversion device with and without ZnO HBL and (b) Photo (under IR illumination) $L-V$ characteristics of PbSe up-conversion device with ZnO HBL under IR illumination with various wavelengths. (Incident NIR power densities at different wavelengths are normalized to 100 μW/cm^2.)

capping group is replaced by a shorter benzenedithiol (BDT) group which is done by chemically treating the PbSe films in BDT.[15,16] In this work, BDT treatment was used in all PbSe nanocrystals films to fabricate the devices.

Figure 3a shows the dark luminance−current−voltage ($L-I-V$) characteristics of the PbSe nanocrystals up-conversion devices with and without the ZnO HBL. The dark current densities of the up-conversion device with the ZnO HBL under forward bias are roughly 2 orders of magnitude lower than that of the device without the ZnO HBL as shown in Figure 3a. These data show that the ZnO layer blocks hole injection from the ITO anode effectively. Low dark current densities are important because they contribute to noise in an up-conversion device. In the absence of IR excitation, the devices without the ZnO HBL behave like normal OLEDs with a high turn-on voltage. The luminance turn-on voltage of the device in the dark is 6 V. The PbSe nanocrystals layer does increase the turn-on voltage of the device, but it is not sufficient to keep the device off under a strong bias. Under infrared irradiation, the device behaves similar to the device operating in the dark, indicating that the device without the ZnO layer does not demonstrate any up-conversion effects (See Figure 1S in the Supporting Information).

On the other hand, the $L-V$ characteristics of the device with the ZnO HBL are measured under different incident NIR illuminations with different power densities at different wavelengths (Figure 2S in the Supporting Information). To compare the $L-V$ characteristics at different wavelengths, Figure 3b shows the luminances normalized to an incident power density of 100 μW/cm^2. Without IR excitation, there is no light emission at voltages up to 17 V, indicating that the ZnO HBL blocks hole

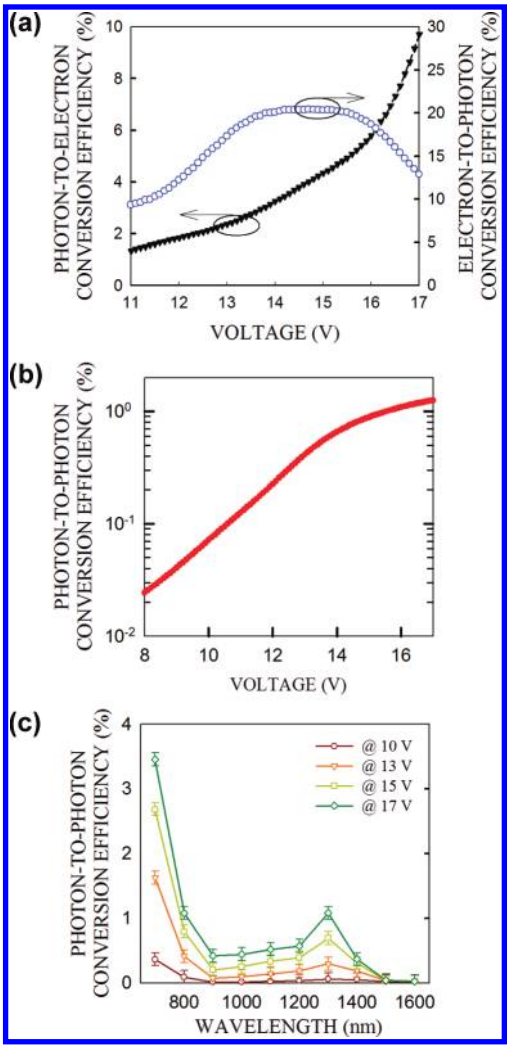

Figure 4. (a) The photon-to-photon conversion efficiency of PbSe up-conversion device as a function of applied voltages. (b) The photon-to-electron conversion efficiency and the electron-to-photon conversion efficiency of PbSe up-conversion device as a function of applied voltages. (c) Spectral photon-to-photon conversion efficiency of PbSe QD up-conversion device as a function of wavelength under different applied voltages.

injection from the ITO electrode effectively as illustrated in Figure 3a. Upon excitation with IR light, the device turned on at voltages between 7 and 8 V along with an onset of green light emission, and the luminance increases with increasing voltage, saturating at high voltages. Under IR illumination, the current through the device is basically limited by injection of photogenerated holes. As the device is illuminated with IR light, photogenerated holes are injected into the OLED resulting in light emission and the number of photogenerated holes depends on the power density of the incident NIR light. The saturation in luminance is due to the maximum hole generation at a given illumination power density. Increasing the illumination power density increases the luminance output of the device. As shown in Figure 3b, excitation at 1.5 μm gives the lowest luminance because of the low absorption coefficient of PbSe nanocrystals at this wavelength and the irradiation at 1.3 μm wavelength gives the highest photoresponse because of the absorption maximum. We should also note that the saturation voltage increases with increasing photoresponse of the device. Since the absorption

dx.doi.org/10.1021/nl200704h |*Nano Lett.* XXXX, XXX, 000–000

Figure 5. The images with and without 1.3 μm NIR illumination in up-conversion device under 15 V.

maximum of the PbSe nanocrystals is at 1.3 μm, the photogenerated hole density is the highest resulting in a higher saturation voltage and a higher luminance maximum. As the illumination wavelength deviates from the maximum, both the saturation voltages and the luminance maxima decrease. These data further confirm that increasing the photogenerated hole density requires higher fields for injection and transport.

The linearity of the photoresponse is shown in Figure 3S (Supporting Information). The photoresponse is linear over 2 decades of power intensities. The IR-to-visible photon-to-photon conversion efficiency (η_{con}) can be calculated by using the equation

$$\eta_{con} = \frac{\text{no. of emitted photons}}{\text{no. of incident photons}} = \frac{\int \frac{\lambda I_{photons}(\lambda)}{R(\lambda)hc}\, d\lambda}{\frac{\lambda_{IR} P_{IR}}{hc}} \quad (1)$$

where h is Planck's constant, c is the speed of light, λ is the wavelength of the emitted light, I_{photo} is the photocurrent measured by the photodetector used for the measurements, $R(\lambda)$ is the responsivity of the photodetector, λ_{IR} is the wavelength of the incident infrared light, and P_{IR} is the incident infrared power.

Both the photon-to-electron (P-E) and electron-to-photon (E-P) conversion efficiencies are shown in Figure 4a. Here, the device dark current has been subtracted to calculate the P-E conversion efficiency. As shown in the figure, the P-E efficiency increases sublinearly with increasing voltage. The increase of the P-E conversion efficiency under low bias (<13 V) is due to increase of injection rate of photogenerated holes into the light emitting layer, and the more rapid increase of the P-E conversion efficiency under higher bias (>16 V) is due to photoconductive gain.[17,18] We have observed photoconductive gain in PbSe QD photodetector, and the details are beyond the scope of this paper and will be reported elsewhere. On the other hand, the E-P conversion efficiency increases with increasing voltage initially, becomes saturated at voltages between 13.5 and 15.5 V, and finally decreases with increasing voltage. The initial increase in the E-P efficiency with voltage is due to the increase in photogenerated hole injection and improvement in charge balance, resulting in a higher quantum efficiency in light emission. At high voltages, while the injection of photogenerated holes becomes saturated, more electrons are injected from the cathode at higher voltages, resulting in a more charge-imbalanced device and hence a lower E-P conversion efficiency. Figure 4b shows the overall photon-to-photon (P-P) conversion efficiency at 1.3 μm IR illumination until the voltage reached 17 V. At voltages beyond 17 V, hole injection is due to photogenerated hole injection and dark hole injection from ITO anode through ZnO HBL. The maximum photon-to-photon conversion efficiency is 1.3% at 17 V as shown in Figure 4b. Similarly, the P-P conversion efficiency has a strong bias dependence due to efficient P-E conversion in the PbSe NIR sensitizing layer.

Figure 4c shows the spectral P-P conversion efficiency as a function of applied voltages. The P-P conversion efficiency spectra are similar to the absorption spectrum of PbSe film as shown in Figure 2. The peak wavelength in conversion efficiency spectra is 1.3 μm and the maximum P-P conversion efficiency at the peak wavelength is 1.3% at 17 V. The low P-P conversion efficiency is due to low absorption coefficients of the PbSe nanocrystal film. The absorption coefficient at the peak wavelength of 1.3 μm is 2.4×10^4 cm^{-1} as shown in Figure 2, and the penetration depth of the 1.3 μm NIR light is calculated to 417 nm, indicating that the 50 nm thick PbSe nanocrystal film used in this device is not thick enough to absorb all the NIR photons. Figure 5 shows the images of the up-conversion device at 15 V with and without 1.3 μm NIR illumination. The switching effect of green light emitting by NIR light irradiation was clearly shown.

In conclusion, we have demonstrated low-cost hybrid up-conversion devices with infrared sensitivity to 1.5 μm by incorporating a colloidal PbSe nanocrystal NIR sensitizing layer with green phosphorescent OLEDs. To keep the device off in the absence of IR excitation, a ZnO nanocrystal hole blocking layer is incorporated in the OLEDs. The maximum photon-to-photon conversion efficiency of an optimized device at peak wavelength of 1.3 μm is 1.3%.

■ ASSOCIATED CONTENT

Supporting Information. Figures showing luminance−current−voltage ($L-I-V$) characteristics of the PbSe nanocrystal up-conversion devices without the ZnO HBL under the dark and the NIR illumination, the $L-V$ characteristics of the PbSe nanocrystal up-conversion devices with the ZnO HBL

dx.doi.org/10.1021/nl200704h |*Nano Lett.* XXXX, XXX, 000–000

under different NIR illumination at various wavelengths, and the luminance at the same applied bias has a linear dependence on the NIR power densities. This material is available free of charge via the Internet at http://pubs.acs.org.

AUTHOR INFORMATION

Corresponding Author
*E-mail: fso@mse.ufl.edu.

ACKNOWLEDGMENT

The authors gratefully acknowledge financial support for the research from DARPA and Nanoholdings.

REFERENCES

(1) Kruse, P. W.; Pribble, F. C.; Schulze, R. G. *J. Appl. Phys.* **1967**, *38*, 1718–1720.
(2) Mita, Y. *Appl. Phys. Lett.* **1981**, *39*, 587–589.
(3) Wang, Y.; Ohwaki, J. *J. Appl. Phys.* **1993**, *74*, 1272–1278.
(4) Russell, K. J.; Appelbaum, I.; Temkin, H.; Perry, C. H.; Narayanamurti, V.; Hanson, M. P.; Gossard, A. C. *Appl. Phys. Lett.* **2003**, *82*, 2960–2962.
(5) Liu, H. C.; Gao, M.; Poole, P. J. *Electron. Lett.* **2000**, *36*, 1300–1301.
(6) Ban, D.; Luo, H.; Liu, H. C.; Wasilewski, Z. R.; SpringThorpe, A. J.; Glew, R.; Buchanan, M. *J. Appl. Phys.* **2004**, *96*, 5243–5348.
(7) Yang, Y.; Shen, W. Z.; Liu, H. C.; Laframboise, S. R.; Wicaksono, S.; Yoon, S. F.; Tan, K. H. *Appl. Phys. Lett.* **2009**, *94*, 093504.
(8) Ni, J.; Tano, T.; Ichino, Y.; Hanada, T.; Kamata, T.; Takada, N.; Yase, K. *Jpn. J. Appl. Phys.* **2001**, *40*, L948–L951.
(9) Chikamatsu, M.; Ichino, Y.; Takada, N.; Yoshida, M.; Kamata, T.; Yase, K. *Appl. Phys. Lett.* **2002**, *81*, 769–771.
(10) Kim, D. Y.; Song, D. W.; Chopra, N.; De Somer, P.; So, F. *Adv. Mater.* **2010**, *22*, 2260–2263.
(11) Ban, D.; Han, S.; Luo, Z. H.; Oogarah, T.; SpringThorpe, A. J.; Liu, H. C. *Appl. Phys. Lett.* **2007**, *90*, 093108−1–3.
(12) Chen, J.; Ban, D.; Feng, X.; Lu, Z.; Fathololoumi, S.; SpringThorpe, A. J.; Liu, H. C. *Appl. Phys. Lett.* **2008**, *103*, 103112.
(13) Sukhovatkin, V.; Musikhin, S.; Gorelikov, I.; Cauchi, S.; Bakueva, L.; Kumacheva, E.; Sargent, E. H. *Opt. Lett.* **2005**, *30*, 171–173.
(14) Sargent, E. H. *Nat. Photonics* **2009**, *3*, 325–331.
(15) Sarasqueta, G.; Choudhury, K. R.; So, F. *Chem. Mater.* **2010**, *22*, 3496–3501.
(16) Sarasqueta, G.; Choudhury, K. R.; Subbiah, J.; So, F. *Adv. Funct. Mater.* **2010**, *21*, 167–171.
(17) Hiramoto, M.; Imahigashi, T.; Yokoyama, M. *Appl. Phys. Lett.* **1993**, *64*, 187–189.
(18) Chen, H.; Lo, M. K. F.; Yang, G.; Monbouquette, H. G.; Yang, Y. *Nat. Nanotechnol.* **2008**, *3*, 543–547.